SUPPLEMENTARY INFORMATION
https://doi.org/10.1038/s41591-018-0044-4

nature medicine

In the format provided by the authors and unedited.

STAT3 labels a subpopulation of reactive astrocytes required for brain metastasis

Neibla Priego[1], Lucía Zhu[1], Cátia Monteiro[1], Manon Mulders[1], David Wasilewski[1,18], Wendy Bindeman[1], Laura Doglio[1,19], Liliana Martínez[1], Elena Martínez-Saez[2,3], Santiago Ramón y Cajal[2,3], Diego Megías[4], Elena Hernández-Encinas[5], Carmen Blanco-Aparicio[5], Lola Martínez[6], Eduardo Zarzuela[7], Javier Muñoz[7], Coral Fustero-Torre[8], Elena Piñeiro-Yáñez[8], Aurelio Hernández-Laín[9], Luca Bertero[10], Valeria Poli[11], Melchor Sanchez-Martinez[12], Javier A. Menendez[13,14], Riccardo Soffietti[15], Joaquim Bosch-Barrera[14,16,17] and Manuel Valiente[1]*

[1]Brain Metastasis Group, Spanish National Cancer Research Centre (CNIO), Madrid, Spain. [2]Pathology Department, Vall d'Hebron Hospital, Barcelona, Spain. [3]Spanish Biomedical Research Network Centre in Oncology (CIBERONC), Barcelona, Spain. [4]Confocal Microscopy Unit, Spanish National Cancer Research Centre (CNIO), Madrid, Spain. [5]Experimental Therapeutics Program, Spanish National Cancer Centre (CNIO), Madrid, Spain. [6]Flow Cytometry Unit, Spanish National Cancer Research Centre (CNIO), Madrid, Spain. [7]ProteoRed-ISCIII. Proteomics Unit, Spanish National Cancer Research Centre (CNIO), Madrid, Spain. [8]Bioinformatics Unit, Spanish National Cancer Research Centre (CNIO), Madrid, Spain. [9]Neuropathology Unit, Hospital Universitario 12 de Octubre Research Institute, Madrid, Spain. [10]Medical Sciences Department, Division of Pathology, University and City of Health and Science University Hospital of Turin, Turin, Italy. [11]Molecular Biotechnology Centre, University of Turin, Turin, Italy. [12]Mind the Byte, Barcelona, Spain. [13]Program Against Cancer Therapeutic Resistance (ProCURE), Metabolism and Cancer Group, Catalan Institute of Oncology, Girona, Spain. [14]Molecular Oncology Group, Girona Biomedical Research Institute (IDIBGI), Girona, Spain. [15]Neuro-Oncology Department, University and City of Health and Science University Hospital of Turin, Turin, Italy. [16]Department of Medical Sciences, Medical School, University of Girona, Girona, Spain. [17]Catalan Institute of Oncology (ICO), Dr. Josep Trueta University Hospital, Girona, Spain. Present address: [18]Institute of Neuropathology, University Medical Center Hamburg-Eppendorf, Hamburg, Germany. [19]Centre for Developmental Neurobiology, King's College London, London, UK. *e-mail: mvaliente@cnio.es

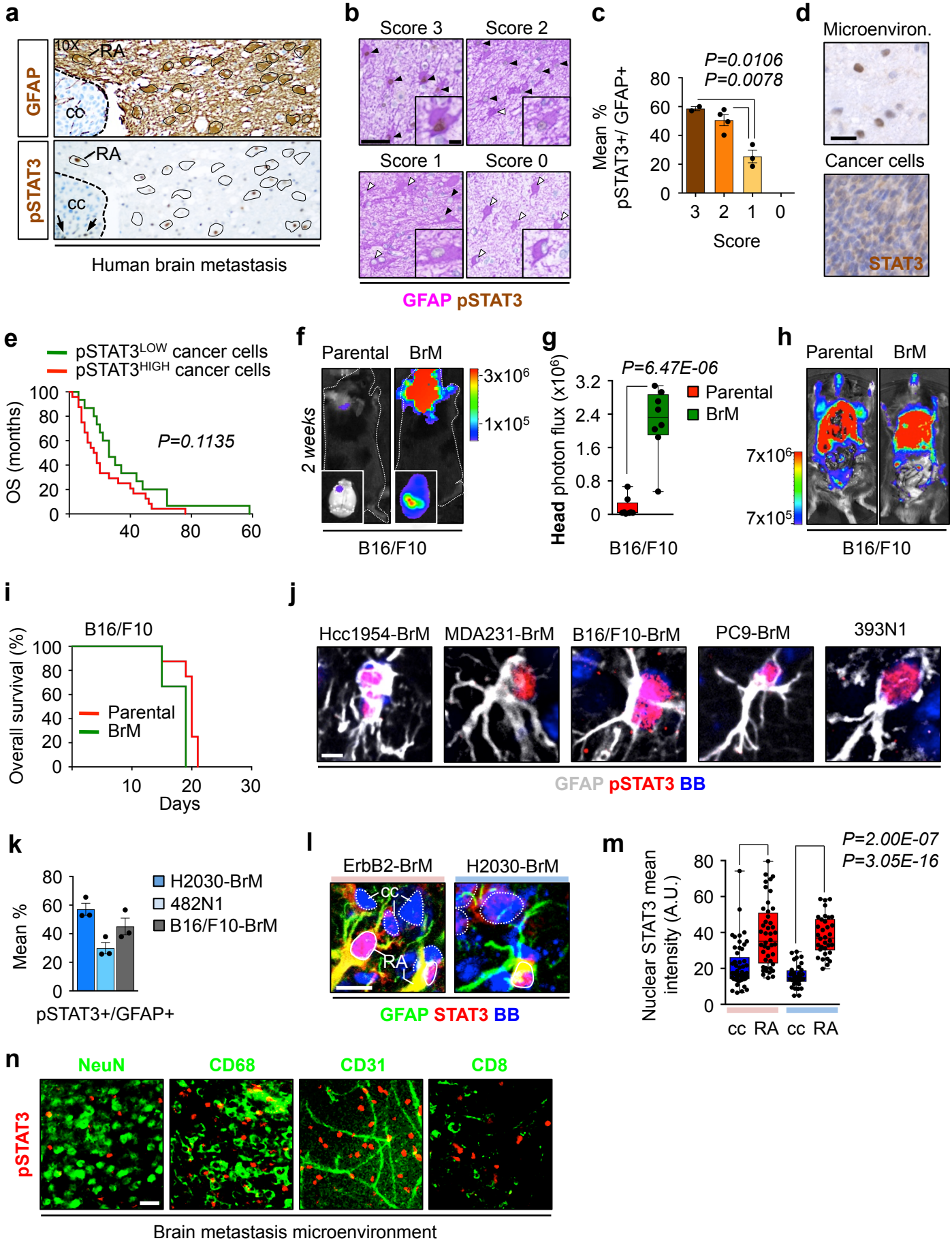

Supplementary Figure 1

Supplementary Figure 1.
a. Immunohistochemistry performed in consecutive paraffin sections of a human brain metastasis shows pSTAT3+ (Tyr705) cells mostly circumscribed to GFAP+ cells. Arrows point to pSTAT3+ cancer cells. **b.** Representative images with different numbers of positive (black arrows) and negative (white arrows) pSTAT3+ reactive astrocytes. High magnification shows differences in intensity. Scale bar: 50 μm, 10 μm (high magnification). **c.** Quantification of the relative abundance of pSTAT3+ reactive astrocytes within GFAP+ cells in previously scored samples using a semiquantitative analysis. Values indicate mean percentage of double positive cells. Error bars, S.E.M. (n=2-3 metastases per category, 73-119 mean GFAP+ cells per metastasis from 2-4 FOV.). P value is calculated using two-tailed t test. **d.** Images of cancer cells or surrounding microenvironment stained with total STAT3 immunohistochemistry. Scale: 25 μm. **e.** Same patients as in Fig.1d were used to generate a survival curve according to the same criteria but scoring pSTAT3 in cancer cells (Score 3, n=7, and 2, n=17) and low (Score 1, n=9, and 0, n=6). P values obtained with log rank (Mantel-Cox) test two-sided. **f,h.** Representative images of wild type C57BL/6 mice two weeks after being inoculated with B16/F10-P or B16/F10-BrM cells intracardiacally. Images showing the BLI of brains (f) and thorax and abdomen (h) are shown. Dotted line indicated the body of mice. **g.** Quantification of bioluminescence imaging (BLI) in the head. Values are shown in box-and-whisker plots where every dot represents a different animal and the line in the box corresponds to the median. Whiskers go from the minimum to the maximum value (n=8 mice per experimental condition). P value is calculated using two-tailed t test. **i.** Survival curve comparing B16/F10-P (n=8) with B16/F10-BrM (n=9) cell lines. P value (*P*=0.0048) is calculated using log rank (Mantel-Cox) test two-sided. **j.** High magnification of reactive astrocytes (RA) with activated STAT3 (Tyr705) in brain metastasis models shown in Fig.1f. Scale bar: 5 μm. **k.** Percentage of double labeled pSTAT3+/ GFAP+ cells. Values indicate mean values ± SEM, 3 metastases were scored in each model. **l.** Representative images of the interface between reactive astrocytes and the metastatic lesion stained with total STAT3. Cc: cancer cells. RA: reactive astrocytes. Scale bar: 12.5 μm. **m.** Quantification of the experiment in (l). Mean intensity of total STAT3 in the nuclei was quantified. Each dot represents a cell (reactive astrocytes, n=34; cancer cells, n=36; 3 metastases in the ErbB2-BrM model; reactive astrocytes, n=44; cancer cells, n=53; 5 metastases in the H2030-BrM model). Values are shown in box-and-whisker plots where every dot represents a cell and the line in the box corresponds to the median. Whiskers go from the minimum to the maximum value. **n.** Double immunofluorescence of pSTAT3 (Tyr705) and different components of the microenvironment surrounding brain metastases. All images correspond to the immediate vicinity of a GFP+ brain metastasis. Scale bar: 25 μm. This result was reproduced in three independent staining with different brains.

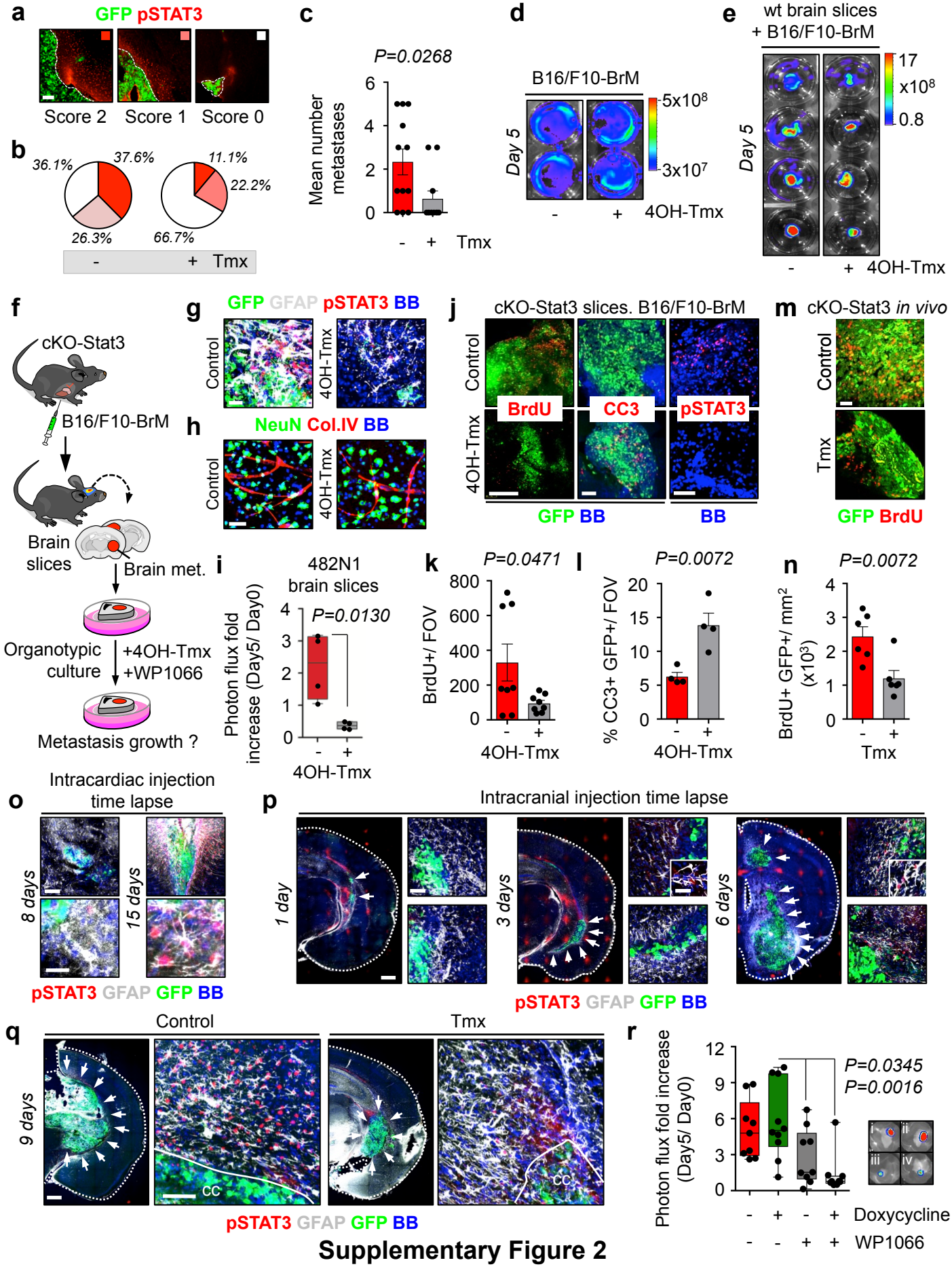

Supplementary Figure 2

Supplementary Figure 2

a. Representative images of GFP+ B16/F10-BrM metastases scored according to the amount of pSTAT3 (Tyr705) signal in the surrounding microenvironment. Colored squares on the top-right corner correspond to the quantification in (b). Scale bar: 100 µm. **b.** Distribution of B16/F10-BrM metastases according to the associated pStat3 signal in the surrounding microenvironment (n=28 control metastases, 7 tamoxifen treated metastases) comparing Tamoxifen treated and untreated cKO-Stat3 mice. **c.** Quantification of the mean number of GFP+ B16/F10-BrM brain metastases found cKO-Stat3 model in Tamoxifen treated or untreated mice. Error bars, S.E.M. (n=11 brains per experimental condition). P value is calculated using two-tailed t test. **d.** 4OH-Tmx (1µM) treatment of B16/F10-BrM cells *in vitro* does not influence their growth rate measured by bioluminescence signal (Control: n=22; mean ± S.E.M. bioluminescence fold increase at day 5= 43.00 ± 6.36; 4OH-Tmx: n=20; mean ± S.E.M. bioluminescence fold increase at day 5= 43.61 ± 7.19). **e.** B16/F10-BrM established brain metastases in wild type mice treated with Tmx (1µM) grow as control brain cultures (n=4 organotypic cultures per experimental condition; Control: mean ± S.E.M. bioluminescence fold increase at day 5= 130.24 ± 53.04; 4OH-Tmx: mean ± S.E.M. bioluminescence fold increase at day 5= 167.74 ± 88.79). **f.** Schema of experimental design. 4OH-Tmx or WP1066 were added to cKO-Stat3 brain slices containing established B16/F10-BrM metastases. **g,h.** Organotypic brain cultures with B16/F10-BrM established brain metastases treated or untreated with 4OH-Tmx. Various cell types could be observed including reactive astrocytes (g), capillaries (h) and neurons (h). Addition of 4OH-Tmx significantly reduced pSTAT3+ reactive astrocytes and tumor burden however with no effect on neurons or capillaries (h). **i.** Quantification of the bioluminescence signal emitted by 482N1 established metastases in cKO-Stat3 mice comparing 4OH-Tmx (1µM) treated and untreated cultures. Values are shown in box-and-whisker plots where every dot represents an individual organotypic culture and the line in the box corresponds to the median. Whiskers go from the minimum to the maximum value (n=4 organotypic cultures per experimental condition). P value is calculated using two-tailed t test. **j.** Representative images of the histology from the experiment shown in (f). CC3: cleaved Caspase 3. pSTAT3 (Tyr705) signal was scored in areas surrounding GFP+ cells. Scale bar: 250 µm (BrdU), 100 µm (CC3), 75 µm (pSTAT3). **k.** Quantification of the mean percentage of BrdU positive cancer cells in cKO-Stat3 organotypic cultures treated with 4OH-Tmx. Error bars, S.E.M. (n=8 field of view from 3 metastases per experimental condition). P value is calculated using two-tailed t test. **l.** Quantification of the mean percentage of cleaved Caspase 3 positive cancer cells in cKO-Stat3 organotypic cultures treated with 4OH-Tmx. Error bars, S.E.M. (n=4 field of view from 2 metastases per experimental condition). P value is calculated using two-tailed t test. **m.** Representative images of the histology from the experiment shown in Fig.2j. Scale bar: 50 µm **n.** Quantification of mean BrdU positive cancer cells in cKO-Stat3 brain with or without Tmx from experiment shown in (j). Error bars, S.E.M. (n=6 metastases per experimental condition, 2 different brains). P value is calculated using two-tailed t test. **o.** Representative images of brain colonization by B16/F10-BrM at two different time points after intracardiac injection. Lower panels show the relative abundance of pStat3+ reactive astrocytes. Scale bar: 100 µm, 20 µm (high magnification). This result was reproduced in three independent staining with different brains. **p.** Representative images of brain colonization by B16/F10-BrM at three different time points after intracranial injection. White arrows indicate the area occupied by the lesion. Two magnifications per time-point show the relative abundance of reactive astrocytes and the gradual emergence of pStat3+. An additional magnification shows individual astrocytes with pStat3. Scale bar: 500 µm, 50 µm (high magnification), 25 µm (individual astrocytes in 3 days and 6 days). This result was reproduced in three independent staining with different brains. **q.** Brains analyzed 6 days after initiation of Tmx treatment (3 days from intracranial injection).

Decreased pSTAT3 signal is evident in reactive astrocytes receiving Tmx. Rest of brains injected intracranially were analyzed at 15 days (Fig.2j-l). Scale bar: 500 μm, 50 μm (high magnification). This result was reproduced in three independent staining with different brains. **r.** Quantification of the bioluminescence signal emitted by iH2030-BrM sh*STAT3* (sh2) cells in each brain slice normalized to the initial value obtained at Day 0, before the addition of any treatment. Values are shown in box-and-whisker plots where every dot represents a different organotypic culture and the line in the box corresponds to the median. Whiskers go from the minimum to the maximum value (No Dox, n=9; Dox, n=10; WP1066, n=9; WP1066+ Dox, n=9 organotypic cultures in each experimental condition, 2 independent experiments). P value is calculated using two-tailed t test. Representative images of brain organotypic cultures with established iH2030-BrM sh*STAT3* (shRNA#2) metastases (Luciferase+) grown *ex vivo* for five days untreated (i) or in the presence of Doxycycline (1 μg/ml) (ii), WP1066 (10 μM) (iii) or both (iv). Bioluminescence scale: minimum: $1x10^7$; maximum.

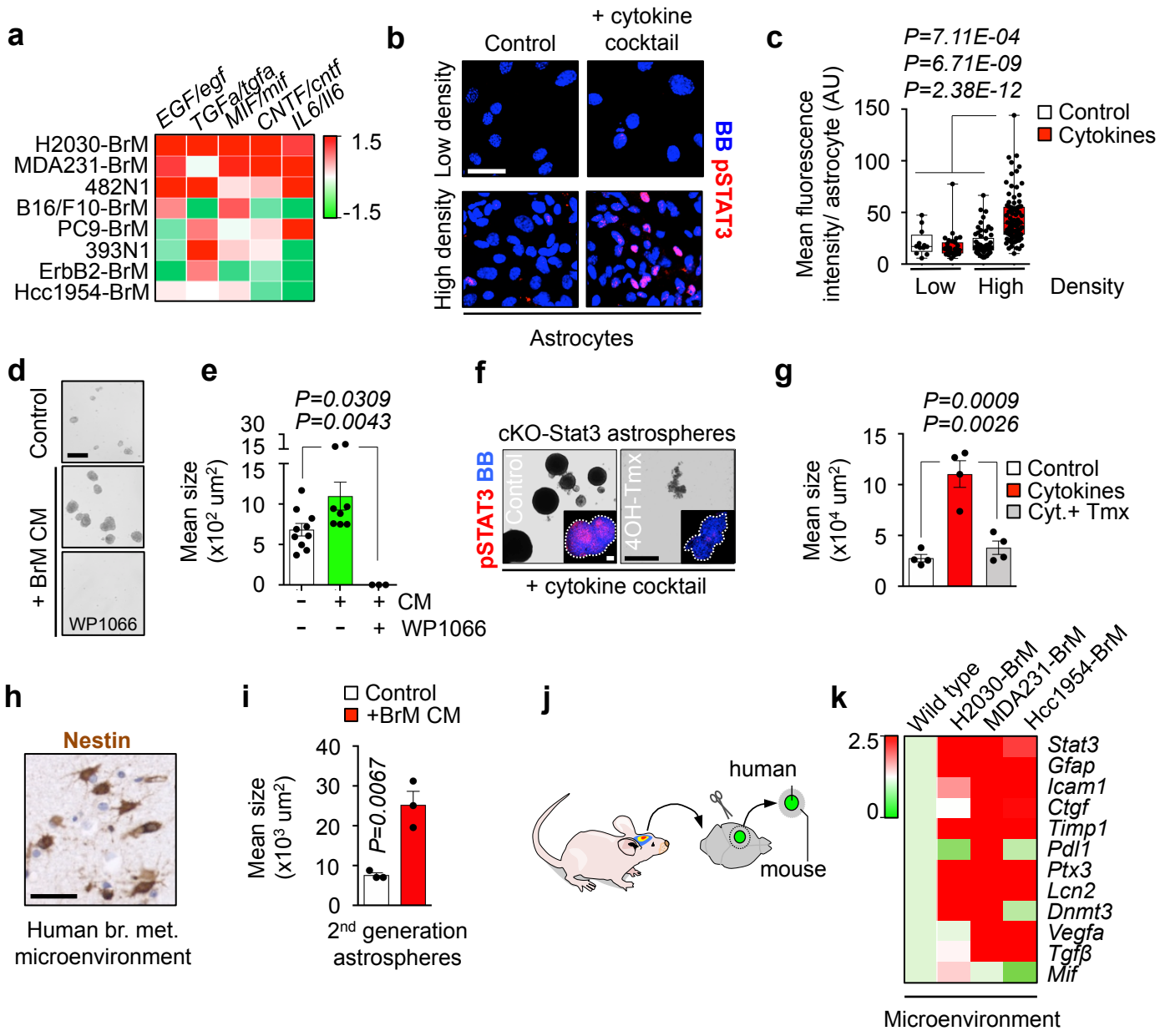

Supplementary Figure 3

Supplementary Figure 3

a. Heatmap indicating human or mouse STAT3 activating cytokines scored in multiple BrM cell lines by qRT-PCR. Level of each cytokine was evaluated in three independent experiments relative to their parental non-brain tropic cell lines. **b.** Representative images of primary astrocyte cultures under adherent conditions with different densities and in the presence or absence of the cytokine cocktail. Scale bar: 30 µm. **c.** Quantification of the experiment in (b). Nuclei from single astrocytes were analyzed for pSTAT3 intensity. Values are shown in box-and-whisker plots where every dot represents a different cell and the line in the box corresponds to the median. Whiskers go from the minimum to the maximum value (High density/ no cytokines: n=62 cells; High density/ cytokines: n=90 cells; Low density/ no cytokines: n=12 cells; Low density/ cytokines: n=31 cells). P value is calculated using two-tailed t test. **d.** Representative images of astrospheres incubated with and without BrM CM. More and bigger astrospheres were found when incubated with BrM CM. Scale bar: 1 mm. **e.** Quantification of the mean size of astrospheres induced by the CM of H2030-BrM cell line. Error bars, S.E.M. (n=10 wells control, 8 wells CM H2030-BrM, 3 wells H2030-BrM with WP1066). P value is calculated using two-tailed t test. **f.** Representative images of cKO-Stat3 derived astrospheres that were generated in the presence or absence of 4OH-Tamoxifen (1µM) and the cytokine cocktail (Fig.3b). Scale bar: 2 mm, high magnification 100 µm. **g.** Quantification of the experiment in (f). Values correspond to the mean size of astrospheres. Error bars, S.E.M. (n=4 wells per condition). P value is calculated using two-tailed t test. **h.** Nestin immunohistochemistry in reactive astrocytes surrounding human brain metastases. Scale bar: 50 µm. **i.** Quantification of the second generation of astrospheres upon addition of BrM CM. Values correspond to the mean size of astrospheres. Error bars, S.E.M. (n=3 wells per condition). P value is calculated using two-tailed t test. **j.** Schema of experimental design. Established metastases from human BrM cell lines were dissected along with the surrounding mouse microenvironment to obtain RNA and perform qRT-PCR. **k.** Heatmap of mouse genes in the microenvironment surrounding resected metastases. Wild type corresponds to a brain without metastases. Values were obtained from analysis of three different resected metastases for each BrM cell line. **l-n.** Triple immunofluorescence of STAT3 downstream targets. ICAM1 co-localizes with pSTAT3 (Tyr705) (l) and CTGF and PD-L1 with GFAP (m,n). White arrows indicate double positive cells. Dotted lines surround established metastases. Cc: cancer cells. Same staining was performed in brains not affected by metastasis (l,m,n). Scale bar: 25 µm (l,m), 75 µm (n), 25 µm (high magnification) (n). These results were reproduced in three independent staining with different brains. **o.** Immunohistochemistry of ICAM1 in human brain metastases samples (Score 0, n=2; Score 1, n=8; Score 2, n=12; Score 3, n=;1). High magnification shows ICAM1+ cell morphology compatible with a reactive astrocyte in the vicinity of cancer cells. Cc: cancer cells. Scale bar: 100 µm, high magnification 25 µm. **p.** Percentage of human brain metastases with ICAM1 positive staining in reactive astrocytes and their immunohistochemistry score.

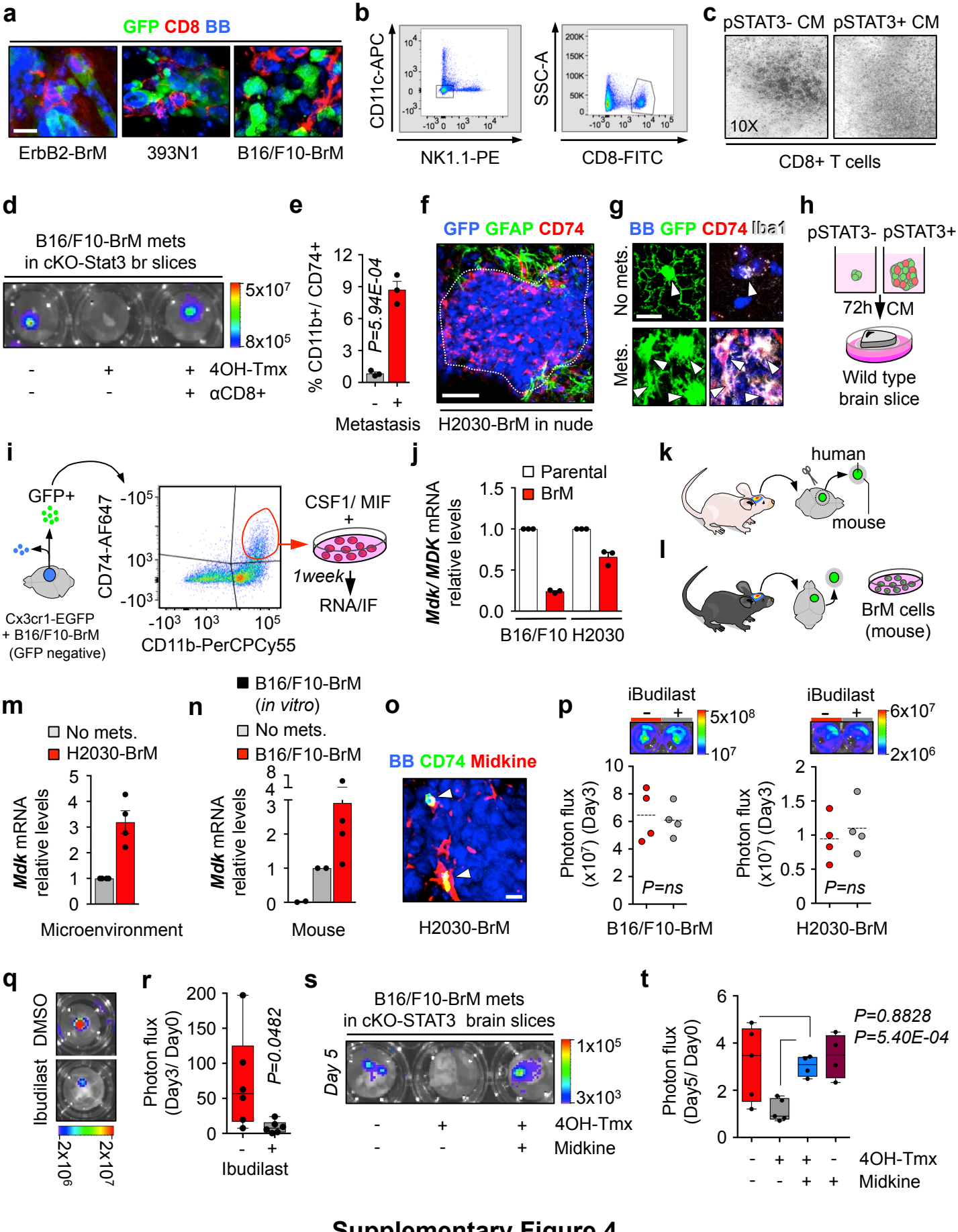

Supplementary Figure 4

Supplementary Figure 4

a. Immunofluorescence against CD8 in established brain metastases from mouse BrM experimental models. Scale bar: 12 μm. This result was reproduced in three independent staining with different brains. **b**. Representative dot plots showing sorted CD11c- NK1.1- CD8+ cells that were used in these experiments. This result was reproduced in four independent experiments. **c.** Representative images of CD8+ T cells after being incubated with CM from astrospheres. This result was reproduced in four independent experiments. **d.** Representative wells containing brain organotypic cultures with established B16/F10-BrM metastases grown *ex vivo* for five days in the presence or absence of 4OH-Tmx (1μM) and anti-CD8 blocking antibody (100 μg/ml). The image shows the bioluminescence intensity in each condition. This result was reproduced in two independent experiments. **e.** Flow cytometry quantification of GFP+ cells obtained from metastasis-free Cx3cr1-EGFP brains and others harboring brain metastases (B16/F10-BrM, GFP negative) according to the population positive for both CD11b and CD74. Values correspond to mean percentage in each experimental condition. Error bars, S.E.M. (n=3 brains per experimental condition). P value is calculated using two-tailed t test. **f.** Double immunofluorescence of GFAP+ reactive astrocytes and CD74+ microglia/macrophages in an established brain metastasis. CD74+ cells infiltrate the lesion. Cancer cells are in blue (GFP). Scale bar: 50 μm. **g.** Images of GFP+ cells from a wild type Cx3cr1-EGFP brain (upper panels) and with a brain harboring B16/F10-BrM metastases (lower panels). Metastasis associated GFP+ cells are located inside the metastasis core. Scale bar: 12.5 μm. **h.** Schema of experimental design. CM: conditioned media from astrospheres. **i.** Cx3cr1-EGFP brains harboring GFP- B16/F10-BrM metastasis were sorted and analyze by flow cytometry. All CD74+/GFP+ cells are CD11b+. CD11b+/CD74+ cells ($CD74^{HIGH}$ and $CD74^{LOW}$) were sorted and cultured with CSF (100ng/ml) and MIF (0.1μg/ml) for 1 week for RNA extraction and immunofluorescence staining. **j.** *Midkine* expression levels in melanoma and lung adenocarcinoma parental (P) and brain tropic (BrM) cell lines. Normalized mean expression values. Three independent cultures per experimental condition. P value is calculated using two-tailed t test (B16/F10: P vs BrM, *P*=1.99E-07; H2030: P vs BrM, *P*=3.31E-03). **k,l.** Schema of experimental design to analyze the expression levels of *Midkine* in xenografts (k) and allografts (l). To compare the expression levels in allografts, a BrM cell line grown *in vitro* was also analyzed. **m,n.** qRT-PCR of microdissected H2030-BrM and B16/F10-BrM brain metastasis surrounding microenvironment shows *Midkine* enriched levels. Normalized mean expression values. Dots correspond to four brains with and without metastases (m) and to two cultures, two brains without metastases and four brains with metastases per experimental conditions (n). **o.** Immunofluorescence of an established H2030-BrM metastasis shows colocalization of Midkine with CD74+ cells. Scale bar: 10 μm. **p.** Representative bioluminescence images and quantification of various BrM cell lines cultured *in vitro* in the absence or presence of ibudilast (50 μM) for 3 days. Dots represent four independent cell cultures (technical replicates). Dotted line indicates the mean value. P value is calculated using two-tailed t test. **q.** Representative wells containing brain organotypic cultures with established B16/F10-BrM metastases grown *ex vivo* for three days in the presence or absence of ibudilast (50μM). The image shows the bioluminescence intensity in each condition. **r.** Quantification of the bioluminescence signal emitted by B16/F10-BrM cells in each brain slice normalized by the initial value obtained at day 0, before the addition of any treatment. Values are shown in box-and-whisker plots where every dot represents a different organotypic culture and the line in the box corresponds to the median. Whiskers go from the minimum to the maximum value (n=6 organotypic cultures per experimental condition). P value is calculated using two-tailed t test. **s.** Representative wells containing brain organotypic cultures with established B16/F10-BrM metastases grown *ex vivo* for five days in the presence or absence of 4OH-Tmx (1μM) and

Midkine (300 ng/ml). The image shows the bioluminescence intensity in each condition. **t.** Quantification of the bioluminescence signal emitted by B16/F10-BrM cells in each brain slice normalized by the initial value obtained at day 0, before the addition of any treatment. Values are shown in box-and-whisker plots where every dot represents a different organotypic culture and the line in the box corresponds to the median. Whiskers go from the minimum to the maximum value (Control: n=5; 4OH-Tmx: n=5; 4OH-Tmx+ Midkine: n=4; Midkine: n=4 organotypic cultures per experimental condition). P value is calculated using two-tailed t test.

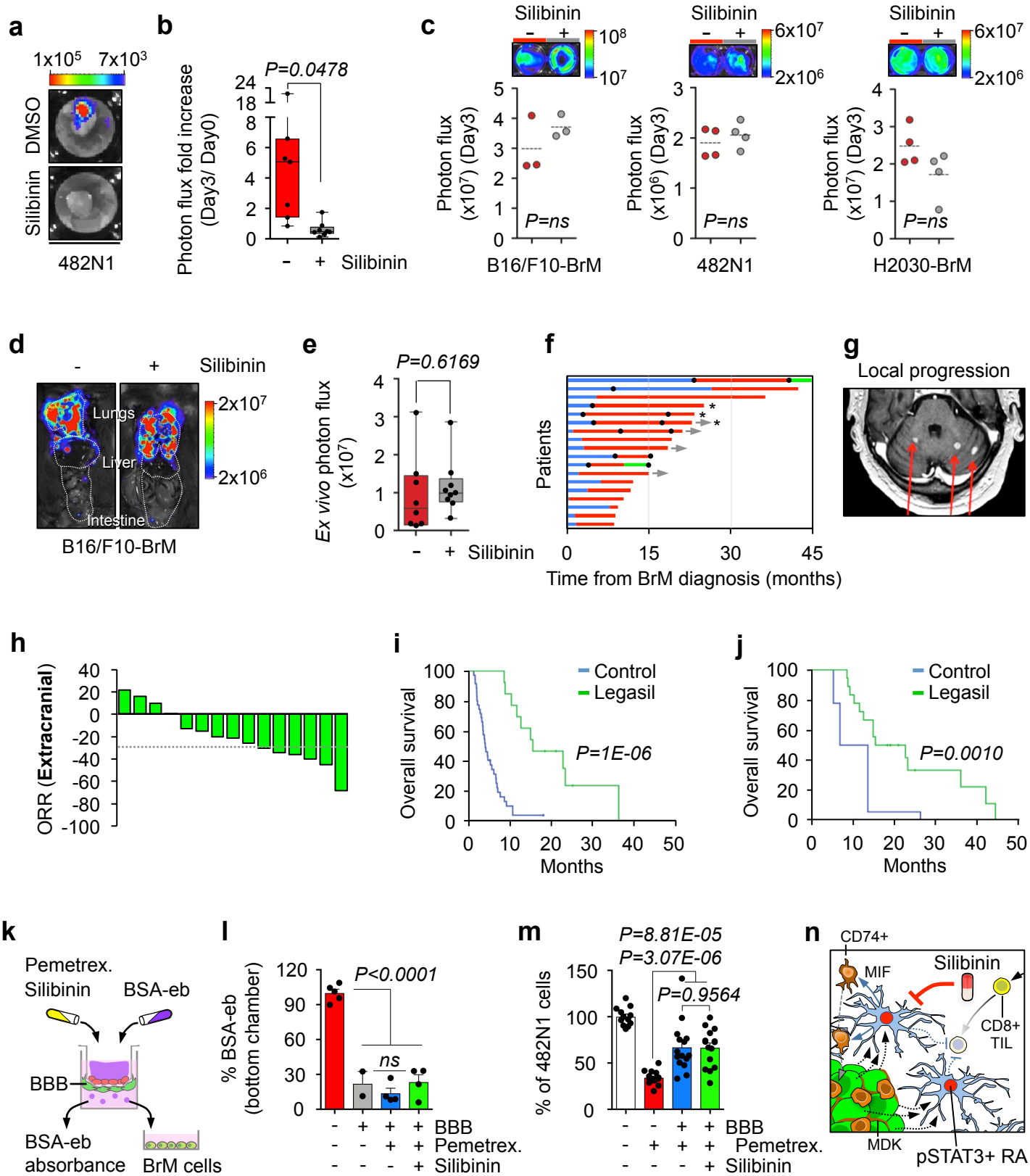

Supplementary Figure 5

Supplementary Figure 5

a. Representative images of brain organotypic cultures with 482N1 established metastases grown *ex vivo* for three days in the presence or absence of silibinin (100 μM). **b.** Quantification of the experiment shown in (a). Values are shown in box-and-whisker plots where every dot represents a different organotypic culture (n=7 per experimental condition) and the line in the box corresponds to the median. Whiskers go from the minimum to the maximum value. P value is calculated using two-tailed t test. **c.** Representative bioluminescence images and quantification of various BrM cell lines cultured *in vitro* in the absence or presence of silibinin (100 μM) for 3 days. Dots represent three (B16/F10-BrM) and four (482N1 and H2030-BrM) independent cell cultures (technical replicates). Dotted line indicates the mean value. P value is calculated using two-tailed t test. **d.** Representative bioluminescence *ex vivo* images of the thorax and abdomen of experiment shown in Fig.5i. **e.** Quantification of the experiment shown in (d). Values are shown in box-and-whisker plots where every dot represents a different animal (Vehicle: n=8; silibinin: n=9) and the line in the box corresponds to the median. Whiskers go from the minimum to the maximum value. P value is calculated using two-tailed t test. **f.** Clinical progression of 18 patients treated with silibinin from diagnosis of the brain metastasis until death. Blue indicates diagnosed brain metastasis without Legasil® treatment. Line is in red when Legasil® was administered. Black circles label progression of local disease in the brain. Green indicates patients who stopped Legasil® because they entered in a clinical trial. Asterisks indicate patients who received Legasil® when under palliative care. Grey arrow indicates patients still alive at data cutoff (1st Sept, 2017). **g.** MRI of a patient treated with Legasil® who progressed locally (red arrows) although remained without clinical symptoms. Newly emerged micro-metastases in the cerebellum remained <1 cm and without associated edema. **h.** Overall response rate (ORR) waterfall plot from extracranial disease (primary tumors and extracranial metastases) in 15 out of the 18 patients with lung cancer metastatic to the brain that received Legasil®. 3 excluded patients did not have extracranial disease (2) or target (measurable) lesion according to RECIST v1.1 criteria. Dotted grey line indicates 30% reduction. **i.** Overall survival (OS) from diagnosis of brain metastasis of 13 patients without alteration in EGFR or ALK who received Legasil® compared to OS of patients treated at the same institution that received systemic therapy but not Legasil® (n=35). P value is calculated by log-rank test two-sided. **j.** Overall survival (OS) from diagnosis of brain metastasis of 18 patients who received Legasil® compared to OS estimated by Lung-molGPA (brain GPA Index) of the same patients. P value is calculated by log-rank test two-sided. **k.** Schema of experimental design. Artificial blood-brain barrier (BBB) containing astrocytes and endothelial cells was incubated with BBB-non-permeable Albumin-evans Blue solution (BSA-eb). The amount of BSA-eb that crossed the BBB in the absence or presence of pemetrexed (50nM), with or without silibinin (100μM), was determined by measuring the absorbance of the dye contained in the bottom chamber media. In other set of experiments the media in the bottom chamber was collected and added to 482N1 lung adenocarcinoma cell line to measure the reduction in cell number. **l.** Mean absorbance of BSA-eb normalized to the levels collected from the bottom chamber in the absence of a BBB. BSA-eb is unable to cross the BBB independently of the treatment. Error bars, S.E.M. (No treatment without BBB: n=5; no treatment with BBB: n=2; pemetrexed with BBB: n=4 w; pemetrexed+ silibinin with BBB: n=4 cell cultures per experimental condition, 2 independent experiments). Absorbance for each culture was determined by measuring three technical replicates. P value is calculated using two-tailed t test (No treatment without BBB vs no treatment with BBB, *P*=1.80E-04; No treatment without BBB vs pemetrexed with BBB, *P*=9.40E-07; No treatment without BBB vs pemetrexed+ silibinin with BBB, *P*=9.36E-06; no treatment with BBB vs pemetrexed with BBB, *P*=0.4261; no treatment with BBB vs pemetrexed+ silibinin with BBB, *P*=0.9089; pemetrexed with BBB vs pemetrexed+ silibinin with BBB, *P*=0.2622). **m.**

Quantification of the mean reduction in cell number normalized to an untreated control. Positive control is pemetrexed-containing media (50 nM). The presence of the BBB limited the ability of pemetrexed to accumulate at the bottom chamber, independently of silibinin, thus limiting capacity to kill cancer cells. Error bars, S.E.M. (No treatment without BBB: n=12 field of view (FOV) from four independent cultures; pemetrexed without BBB: n=15 FOV from five independent cultures; pemetrexed with BBB: n=15 FOV from five independent cultures; pemetrexed+ silibinin with BBB: n=15 FOV from five independent cultures, 2 independent experiments). P value is calculated using two-tailed t test. **n.** Model summarizing main findings regarding the involvement of pSTAT3+ RA in brain metastasis, their potential pro-metastatic functions and the specific therapy. TIL: tumor infiltrating lymphocytes.

Supplementary table 1. Brain metastasis samples analyzed for pSTAT3 in reactive astrocytes

Sample	1ry tumor	Subtype	Oncogenomics	pSTAT3 IHC in RA	Survival (months)
#1	Lung	Adenocarcinoma	EGFRwt/ ALKwt	0	32
#2	Lung	Adenocarcinoma	ND	0	27
#24	Lung	Adenocarcinoma	EGFRwt/ ALKwt	0	
#25	Lung	Adenocarcinoma	**EGFRmut**/ ALKwt	0	
#26	Lung	Adenocarcinoma	EGFRwt/ ALKwt	0	
#27	Lung	Adenocarcinoma	EGFRwt/ ALKwt	0	
#3	Lung	Squamous cell carcinoma	**EGFRmut**/ ALKwt	1	4
#4	Lung	Adenocarcinoma	EGFRwt/ ALKwt	1	21
#5	Lung	Adenocarcinoma	EGFRwt/ ALKwt	1	9
#6	Lung	Adenocarcinoma	**EGFRmut**/ ALKwt	1	
#7	Lung	Squamous cell carcinoma	ND	1	20
#8	Lung	Adenocarcinoma	EGFRwt/ ALKwt	1	3
#9	Lung	Adenocarcinoma	EGFRwt/ ALKwt	1	5
#10	Lung	Adenocarcinoma	**EGFRmut**	1	38
#11	Lung	Adenocarcinoma	ND	1	5
#12	Lung	Adenocarcinoma	ND	1	32
#13	Lung	Squamous cell carcinoma	ND	1	4
#14	Lung	ND	ND	1	25
#28	Lung	Adenocarcinoma	EGFRwt/ ALKwt	1	
#29	Lung	Adenocarcinoma	EGFRwt/ ALKwt	1	
#30	Lung	Adenocarcinoma	ALKwt	1	
#31	Lung	Adenocarcinoma	ND	1	
#32	Lung	Adenocarcinoma	EGFRwt/ ALKwt/ ROSwt	1	
#33	Lung	Epidermoid carcinoma	ND	1	
#34	Lung	Adenocarcinoma	ND	1	
#15	Lung	Adenocarcinoma	EGFRwt/ ALKwt	2	5
#16	Lung	Adenocarcinoma	EGFRwt/ ALKwt	2	13
#17	Lung	Squamous cell carcinoma	ND	2	22
#18	Lung	Squamous cell carcinoma	ND	2	11
#19	Lung	Adenocarcinoma	ND	2	6
#20	Lung	Adenocarcinoma	ALKwt/ ROSwt	2	1
#21	Lung	ND	ND	2	13
#35	Lung	Adenocarcinoma	EGFRwt/ ALKwt	2	
#36	Lung	Adenocarcinoma	ND	2	
#37	Lung	Adenocarcinoma	EGFRwt/ ALKwt/ ROSwt	2	
#38	Lung	Squamous cell carcinoma	ND	2	
#39	Lung	Carcinoma	ND	2	
#22	Lung	Adenocarcinoma	EGFRwt/ ALKwt	3	9
#23	Lung	Adenocarcinoma	EGFRwt/ ALKwt/ ROSwt	3	9
#40	Lung	Adenocarcinoma	ND	3	
#41	Lung	Large cell neuroendocrine carcinoma	EGFRwt/ ALKwt/ ROSwt	3	
#42	Lung	Undifferentiated carcinoma	EGFRwt/ ALKwt/ ROSwt	3	
#43	Lung	Adenocarcinoma	ND	3	
#44	Lung	Adenocarcinoma	ND	3	
#45	Breast	Adenocarcinoma	ER+/PR+/**HER2+**	0	8
#46	Breast	Adenocarcinoma	ND	0	59
#62	Breast	Adenocarcinoma	ER-/PR-/**HER2+**	0	
#63	Breast	Adenocarcinoma	ER+/PR-/HER2-	0	
#47	Breast	Adenocarcinoma	ER+/PR+/HER2-	1	10
#48	Breast	Adenocarcinoma	**ER-/PR-/HER2-**	1	10
#49	Breast	Adenocarcinoma	ER-/PR+/HER2-	1	3
#50	Breast	Adenocarcinoma	ER+/PR+/HER2-	1	24
#51	Breast	Adenocarcinoma	ER+/PR+/**HER2+**	1	15
#52	Breast	ND	ND	1	26
#64	Breast	Adenocarcinoma	ER-/PR+/**HER2+**	1	
#65	Breast	Adenocarcinoma	ER-/PR-/**HER2+**	1	
#66	Breast	Adenocarcinoma	ER+/PR+/**HER2+**	1	
#67	Breast	Adenocarcinoma	ER-/PR+/**HER2+**	1	
#68	Breast	Adenocarcinoma	ER-/PR-/**HER2+**	1	
#69	Breast	Adenocarcinoma	ND	1	
#70	Breast	Adenocarcinoma	ND	1	
#71	Breast	Adenocarcinoma	ER+/PR-/**HER2+**	1	
#53	Breast	Adenocarcinoma	ER+/PR+/**HER2+**	2	13
#54	Breast	Adenocarcinoma	ER-/PR-/**HER2+**	2	4
#55	Breast	Adenocarcinoma	**ER-/PR-/HER2-**	2	3
#56	Breast	Adenocarcinoma	ER+/PR+/HER2-	2	6
#57	Breast	Adenocarcinoma	ER-/PR-/**HER2+**	2	16
#72	Breast	Adenocarcinoma	**ER-/PR-/HER2-**	2	
#73	Breast	Adenocarcinoma	**ER-/PR-/HER2-**	2	
#74	Breast	Adenocarcinoma	ER+/PR+/**HER2+**	2	
#75	Breast	Adenocarcinoma	ND	2	
#76	Breast	Adenocarcinoma	ER+/PR-/**HER2+**	2	
#77	Breast	Adenocarcinoma	ND	2	
#78	Breast	Adenocarcinoma	**ER-/PR-/HER2-**	2	
#58	Breast	Adenocarcinoma	ER+/PR+/**HER2+**	3	8
#59	Breast	Adenocarcinoma	ER-/PR-/**HER2+**	3	7
#60	Breast	Adenocarcinoma	ER+/PR+/HER2-	3	17
#61	Breast	Adenocarcinoma	**HER2+**	3	10
#79	Breast	Adenocarcinoma	ER-/PR-/**HER2+**	3	
#80	Breast	Adenocarcinoma	**ER-/PR-/HER2-**	3	
#81	Breast	Adenocarcinoma	ER+/PR-/**HER2+**	3	
#82	Breast	Adenocarcinoma	ND	3	
#83	Breast	Adenocarcinoma	ER+/PR-/**HER2+**	3	
#84	Breast	Adenocarcinoma	**ER-/PR-/HER2-**	3	
#85	Melanoma		ND	1	
#86	Melanoma		ND	1	
#87	Kidney	Carcinoma	ND	1	
#88	GI	Adenocarcinoma	ND	3	
#89	GI	Adenocarcinoma	ND	3	
#90	Unknown	ND	ND	1	
#91	Unknown	Carcinoma	ND	2	

ND: not determined

Supplementary table 2. Brain tropic cancer cell lines

Brain tropic cells	Species	Cancer subtype/ Main oncogenic mutations.	Study	
H2030-BrM	Human	*KRAS^{G12C}; TP53^{G262V}*	Nguyen et al.	**Lung** adenocarcinoma
PC9-BrM	Human	*EGFR$^{\Delta E746\text{-}A750}$*	Nguyen et al.	
482N1	Mouse	*Kras^{G12D}; Tp53^{null}*	Valiente et al.	
393N1	Mouse	*Kras^{G12D}; Tp53^{null}*	Valiente et al.	
MDA231-BrM	Human	Triple negative. Basal	Bos et al.	**Breast** adenocarcinoma
Hcc1954-BrM	Human	ERBB2+	Maladi et al.	
ErbB2-BrM	Mouse	ErbB2+	Valiente et al.	
B16/F10-BrM	Mouse	*Cdkn2a^{null}; Tp53^{N127D}; Pten$^{A39V/T131P}$*	This mansucript	**Melanoma**

Supplementary Table 3. Binding energies of silibinin to native and mutant STAT3.

Docking binding energies of silibinin against human homology models (HM) of the SH2 domain of native STAT3 and A662C/N664C mutant STAT3C.

	A662C/N664C mutant STAT3C HM docking (kcal/mol) R0/R1[±]			
Native STAT3 HM docking (kcal/mol) R0/R1[±]	**Frame 1**	**Frame 800 (pose 1)**	**Frame 800 (pose 3)**	**Frame 2000**
-5.6/-5.9	-5.9/-5.9	-4.0/-3.9	-3.9/-3.9	-7.2/-7.2

Table summarizes the binding energies of the docking calculations realized with silibinin over selected snapshots of a human HM of the SH2 domain of native STAT3 and A662/N664C mutant STAT3C. Each calculation was performed twice (R0, R1) to avoid false positives. [±]The more negative the binding energy, the more plausible the interaction.

MM/GBSA-based binding energy rescoring calculations of silibinin against human HM of the SH2 domain of native STAT3 and A662C/N664C mutant STAT3C.

	A662C/N664C mutant STAT3C HM MM/GBSA (kcal/mol)[±]			
Native STAT3 HM MM/GBSA (kcal/mol) [±]	**Frame 1**	**Frame 800 (pose 1)**	**Frame 800 (pose 3)**	**Frame 2000**
-20.009	-11.226	-16.892	-24.218	-28.221

Table summarizes the MM/GBSA rescored binding energies of the MDS analyses realized with silibinin over selected snapshots of a human HM of the SH2 domain of native STAT3 and A662/N664C mutant STAT3C. [±]The more negative the binding energy, the more plausible the interaction.

Supplementary table 4. Patients treated with and without Legasil®.

Data are n (%). BM = Brain metastasis. GPA=graded prognostic assessment. PS=performance status. Due to a retrospective analysis, we report statistical analysis of variables between groups in order to detect possible bias. Student's t test (two-sided) for variables median age, number of BM, an size of biggest BM, and a chi-squared test for the rest of the variables (sex, karnofsky PS, extracraneal metastases, histology, BM status, GPA prognostic class and Gene status) were used. Significance was set at *P< 0.05*.

	Legasil® Group (n=18)	**Control Group** (n=38)	**p-value**
Sex			*=0.457*
Male	11 (61%)	27 (71%)	
Female	7 (39%)	11 (29%)	
Age (y)			*=0.986*
<70	16 (89%)	33 (87%)	
>70	2 (11%)	5 (13%)	
Median (Range)	62 (35-80)	61.5 (35-84)	
Karnofsky PS			***=0.008****
>70%	8 (44%)	27 (71%)	
≤70%	10 (56%)	11 (29%)	
Extracranial metastases			*=0.693*
Present	16 (89%)	35 (92.1%)	
Absent	2 (11%)	3 (7.9%)	
Histology			*=0.725*
Small cell	2 (11%)	5 (13.2%)	
Squamous	1 (5.5%)	6 (15.8%)	
Adenocarcinoma	14 (78%)	25 (65.8%)	
Other	1 (5.5%)	2 (5.2%)	
BM status			*=0.394*
Newly diagnosed	13 (72%)	23 (60.5%)	
Progressive disease	5 (28%)	15 (39.5%)	
GPA prognostic class			*= 0.066*
3.5-4.0	0	1 (2.6%)	
2.5-3.0	1 (5.5%)	3 (7.9%)	
1.5-2.0	8 (44.5%)	18 (47.4%)	
0.0-1.0	9 (50%)	16 (42.1%)	
Gene status			***=0.047****
EGFR pos	4 (22%)	2 (5.2%)	
ALK pos	1 (5%)	1 (2.6%)	
Number of BM			*=0.484*
Median (Range)	4 (1-20)	3 (1-20)	
Size of biggest BM (mm)			*=0.806*
Median (Range)	26 (10-65)	26.5 (6-47)	

* Statistical significant differences (*P<0.05*)

Supplementary table 5. Systemic therapy administered to patients.

	Legasil® Group	Control Group
Previous line to brain M1	**5 (28%)**	**5 (13%)**
Carboplatin-vinorelbine & lung radiotherapy (stage III)	3	3
Cisplatin-pemetrexed (stage IV)	1	-
Gefitinib (stage IV)	1	-
Carboplatin-paclitaxel & lung radiotherapy (stage III)	-	2
1st line	**18 (100%)**	**33 (87%)**
Carboplatin-pemetrexed	8	13
Cisplatin-pemetrexed	1	2
Pemetrexed	3	1
Carboplatin-etoposide	2	5
EGFR TKI	3	2
Carboplatin-gemcitabine	1	4
Cisplatin-vinorelbine	-	5
Carboplatin-paclitaxel	-	1
2nd line	**14 (78%)**	**10 (26%)**
Carboplatin-pemetrexed	3	1
Pemetrexed	2	1
Docetaxel	3	2
Docetaxel-nintedanib	1	-
Nivolumab	1	-
Carboplatin-gemcitabine	1	1
Carboplatin-etoposide	1	3
Crizotinib	1	2
Erlotinib	1	-
3rd line	**6 (33%)**	**3 (8%)**
Carboplatin-gemcitabine	1	-
Erlotinib	1	-
Docetaxel-nintedanib	1	-
3rd generation EGFR TKI*	1	-
3rd generation ALK TKI*	1	-
Nivolumab	1	1
Topotecan	-	2
4th line	**2 (11%)**	**1 (3%)**
Pemetrexed	1	-
Erlotinib	1	-
Paclitaxel	-	1

* Treatment received in a clinical trial, the patient stopped silibinin supplementation before inclusion to the clinical trial and during all the treatment with this experimental drug according to study protocol.

Supplementary table 6. Therapeutic schedule in patients treated with Legasil®.

Patient	Previous extracranial treatment	Start	Progressive disease	BM diagnosis	Neurosurgery	Other treatment	Start WBRT	End WBRT	1st line	Start	PD	Type
#1				day 0			1.3	1.8	Cisplatin+Pemetrexed	0.1	21.0	Extracraneal
#2				day 0			0.9	1.4	Gefitinib	1.2	9.5	Brain
#3	Cisplatin+pemetrexed	-12.8	Extracranial & brain	day 0			1	1.5	Carboplatin+Pemetrexed	0.5	22.2	Extracranial & brain
#4				day 0			0.5	1	Carboplatin+Pemetrexed	1.2	3.2	Brain
#5				day 0			1.2	1.7	Pemetrexed	2.3	3.9	Extracranial & brain
#6	Carboplatin+Vinorelbine+Lung RT	-6.0	Brain	day 0	Yes (1,4 months)	SBRT (8,5 months)	2.5	3	Pemetrexed	3.3	4.5	Brain
#7	Carboplatin+Vinorelbine+Lung RT	-3.7	Brain	day 0		SBRT (12,5 months)	2.6	3.1	Carboplatin+Pemetrexed	17.4	19.1	Brain
#8	Carboplatin+Vinorelbine+Lung RT	-17.3	Brain	day 0	Yes (0,6 months)		2.9	3.4	Carboplatin+Pemetrexed	3.7	8.7	Brain
#9				day 0			0.4	0.9	Afatinib	0.9	16.2	No
#10				day 0			5.2	5.7	Erlotinib	1.2	2.5	Extracranial & brain
#11				day 0			1.5	2	Carboplatin+Etoposide	0.8	9.3	Extracraneal
#12				day 0			2.3	2.8	Carboplatin+Pemetrexed	2.4	18.5	No
#13				day 0			1	1.5	Carboplatin+Etoposide	2.4	3.5	Extracraneal
#14				day 0	Yes (0,3 months)		0.9	1.4	Carboplatin+Gemcitabine	1.9	8.0	Extracraneal
#15				day 0			1.2	1.7	Carboplatin+Pemetrexed	0.6	7.6	Extracraneal
#16	Gefitinib	-3.3	Brain	day 0			0.5	1	Pemetrexed	0.5	2.8	Extracraneal
#17				day 0			0.9	1.4	Carboplatin+Pemetrexed	0.7	7.6	Extracraneal
#18				day 0			2.2	2.7	Carboplatin+Pemetrexed	0.9	5.8	Extracraneal

Patient	2nd line	Start	PD	3rd line	Start	PD	4th line	Start	PD	Start Legasil	Stop legasil	OS	Alive/ Dead
#1	Crizotinib	21.5	42.4	Ceritinib	43.4	44.7				23.2	43	44.75	Dead
#2	Carboplatin+Pemetrexed	10.1	22.8	Erlotinib	23.3	42.4				26.4	42.41	42.41	Dead
#3	Carboplatin+Gemcitabine	22.6	26.7	Nivolumab	27.7	33.5				5.4	36.3	36.3	Dead
#4	Pemetrexed	4.8	12.0	Docetaxel+Nintedanib	12.5	17.3	Pemetrexed	18.8	20.5	3.4	23.39	23.39	Dead
#5	Docetaxel	6.7	9.1	Carboplatin+Gemcitabine	9.4	16.6	Erlotinib	17.5	19.1	4.9	22.83	22.83	Dead
#6	Pemetrexed	3.0	23.3							4.6	25.1	25.1	**Alive**
#7										1.1	21.1	21.1	**Alive**
#8	Carboplatin+Pemetrexed	9.4	12.5							9.1	15.54	15.54	Dead
#9										2.8	19.2	19.2	**Alive**
#10	Carboplatin+Pemetrexed	3.0	7.6	Rociletinib CT	10.4	14.9				3.7	10	14.98	Dead
#11	Carboplatin+Etoposide	9.4	12.9							2.1	14.46	14.46	Dead
#12										3.1	18.5	18.5	**Alive**
#13										3.8	11.66	11.66	Dead
#14	Nivolumab	8.7	12.0							6.2	11.24	12.06	Dead
#15	Docetaxel	8.6	9.0							0.3	10.35	10.35	Dead
#16	Erlotinib	6.5	9.3							7.9	9.33	9.33	Dead
#17	Docetaxel	8.3	8.8							1.5	8.84	8.84	Dead
#18	Docetaxel-Nintedanib	6.1	7.5							1.7	8.61	8.61	Dead